Public

Report

Document ID	Version	Status		Reg no	Page
1419643	1.0	Approved			1 (33)
Author				Date	
Jan Hernelind/5T Engineeering AB				2014-01-21	
Reviewed by				Reviewed date	
Sanja Trkulja (QA)				2014-02-05	
Approved by				Approved date	
Jan Sarnet				2014-02-05	

Analysis of canister with unfavourable pressure load

Abstract

The purpose of this study is to investigate how swelling of the bentonite during the water saturation phase may affect the canister when the swelling is initiated. The swelling is caused by water inflow from the surrounding rock and creates a radial swelling pressure which acts on the outer surface of the copper shell. Two extreme and pessimistic assumptions are studied:

- One assumed horizontal crack close to the copper lid flange which implies a radial swelling pressure at the outer surface of the flange at the same time it is pessimisticly assumed that no radial counter swelling pressure will be build up during the water saturation phase as the recess in the copper lid can't be fully filled with bentonite along the periphery. Furthermore, it can't be excluded that an axial swelling pressure also develops acting on the lid and interacts with the radial pressure.

- Several evenly distributed horizontal cracks which imply a radial swelling pressure at the outer surface of the copper shell and at the same time generates an axial expansion of the bentonite which implies axial shear stresses at the outer surface of the copper shell. Same assumptions regarding counter pressure and vertical pressure at the lid as in the previous case.

Despite the various pessimistic assumptions the simulations shows that the plastic strain in the copper shell is not exceeding 6.2% which is considerably lower than the strains the copper shell can withstand. The "Design report for the canister" (Raiko et al. 2010) specifies the criteria to more than 80% effective strain in tension.

Sammanfattning

Syftet med denna studie är att undersöka hur bentonitens svällning under vattenmättnadsfasen kan påverka kapseln när svällningen initieras. Svällningen orsakas av vatteninflöde från det närliggande berget och skapar ett radiellt svälltryck som verkar på utsidan av kopparhöljet. Två extrema och pessimistiska antaganden studeras:

- En antagen horisontell spricka nära kopparlockets fläns som ger ett radiellt svälltryck på utsidan av flänsen samtidigt som det pessimistiskt antas att inget radiellt mottryck byggs upp under vattenmättnadsfasen då urtaget i kopparlocket ej helt kan fyllas med bentonit längs periferin. Dessutom kan inte uteslutas att ett axiellt svälltryck också utvecklas på locket och samverkar med det radiella trycket.

PDF rendering: DokumentID 1419643, Version 1.0, Status Godkänt, Sekretessklass Öppen

- Ett antal jämnt fördelade horisontella sprickor som ger ett radiellt svälltryck på utsidan av kopparskalet och en samtidig axiell expansion av bentoniten som medför axiella skjuvspänningar på kopparskalets utsida. Samma antaganden om mottryck och vertikalt tryck på locket som i föregående fall.

Trots de olika pessimistiska antagandena visar simuleringarna att den plastiska töjningen i kopparhöljet uppgår högst till 6.2% som är avsevärt lägre än de töjningar som kopparhöljet klarar. I "Design report for the canister" (Raikko et al. 2010) anges kriteriet till mer än 80% effektiv töjning i drag.

Contents

1   Introduction

The swelling process under the water saturation phase could affect the top of the canister when the bentonite swelling starts close to the top of the canister. This could be caused by water inflow from the nearby surrounding rock. The swelling could create a temporary radial swelling pressure acting on the outside of the copper lid flange. No counter pressure is assumed to occur as the recess in the lid cannot be filled completely with bentonite. In addition a vertical pressure on the lid due to swelling effects could not be excluded and this pressure could interact with the radial pressure and imply bending of the copper shell at the top.

To investigate how an unfavourable swelling process affects the stresses and strains in the copper shell two cases have been studied, see also Chapter 6 "Boundary conditions and loading":

1) External pressure (corresponding to the swelling pressure only at the copper shell lid and the outer copper shell top). Model name Isostat_radial_pressure1, Figure 1-1 (left).
2) Gravity load, external pressure on the copper shell lid and the outer vertical surface of the copper shell. Also the effect of swelling bentonite causing friction forces in vertical direction on the copper shell is included. Model name Isostat_radial_pressure2, Figure 1-1 (right).
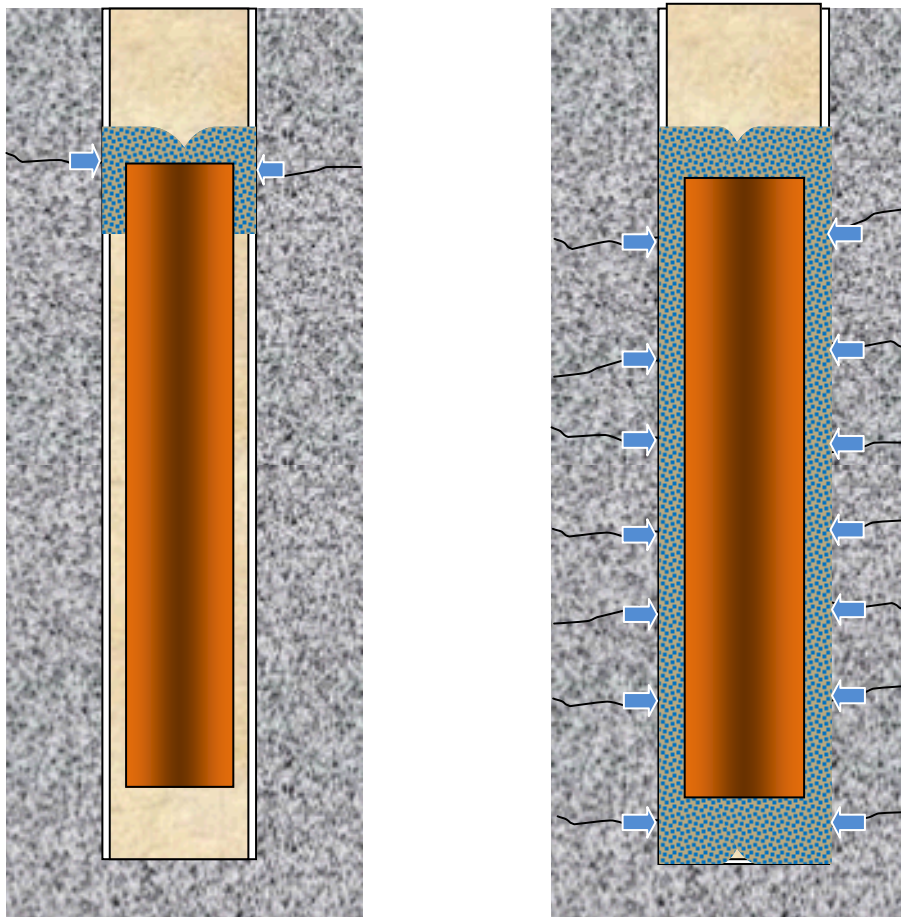
Figure 1-1. *Physical illustration of the studied load cases. Left plot, swelling from water flow in a horizontal crack cutting through the deposition hole at canister top.   Right plot, swelling from water flow in several horizontal cracks cutting through the deposition hole.*

Context for this report

The insert (nodular cast iron) material properties are based on experimental results. The steel lid and the steel cassette material properties are based on supplier's available information. The copper shell material model is based on a creep model developed by Rolf Sandström (Sandström and Andersson 2008, Jin et al. 2008, Sandström et al. 2009).

This report summarizes the results for analyses performed by using an axi-symmetric approach where the only loads applied are gravity and swelling pressure from the buffer.

Factors considered in the simulation

The following factors are taken into account in the simulations.

Canister geometry
- An imperfect weld with a root defect with 3 mm in size.

Load evolution
- Isostatic pressure from buffer swelling caused by the water saturation phase. The highest swelling pressure occurs for bentonite with density 2050 kg/m^3 with a magnitude of 12.3 MPa (Börgesson et al. 2010).

- The swelling pressure is applied to the copper shell (two cases).

- The buffer swelling along the canister also creates shear forces on the outer surface of the copper shell. However, the shear stress is limited to 1.75 MPa (Börgesson et al. 2010) which corresponds to the shearing capacity of the buffer. The distribution of the axial shear stresses needs to be in equilibrium (if the gravity load is neglected half length of the copper shell surface have shear stresses pointing upwards and the other half have shear stresses pointing downwards). The most conservative assumption is that the shear stress reaches its maximum value and has a constant magnitude along the surface of the canister, 1.75 MPa.

2 Simulation strategy

The performed simulations are all based on the same geometry which consists of a copper shell, canister (iron), lid (steel) as a simplified axi-symmetric model.   The insert is assumed to completely consist of solid cast. All analyses are performed using the '*static'-procedure in Abaqus which means that only displacement degree of freedoms are used and that inertia loads are neglected.

3   Geometry definitions and meshes

The geometry consists of the insert , the insert lid and the surrounding copper shell. The geometry is based on CAD-geometries received from SKB "Ritningförteckning för kapselkomponenter", (SKBdoc 1203875) and should therefore correspond to the current design. The geometry of the FSW (Friction Stir Welding) weld is modelled by an axial slit and a root defect in radial direction (radial slit).

An axi-symmetric approach is used since the main focus in this study is on the copper shell and the insert stiffness could be approximated by an axi-symmetric geometry based on previous analyses.

The axi-symmetric model neglects the steel cassettes and thus only consists of the insert (made of nodular cast iron), the insert lid (made of steel) and the surrounding copper shell; see Figures 3-1 to 3-3. The mesh is then generated by 2-dimensional solid elements, mainly 4-noded quadrilateral elements with reduced integration (CAX4R). The axi-symmetric model size is defined by about 12,000 elements and 13,000 nodes (total number of variables about 34,000).
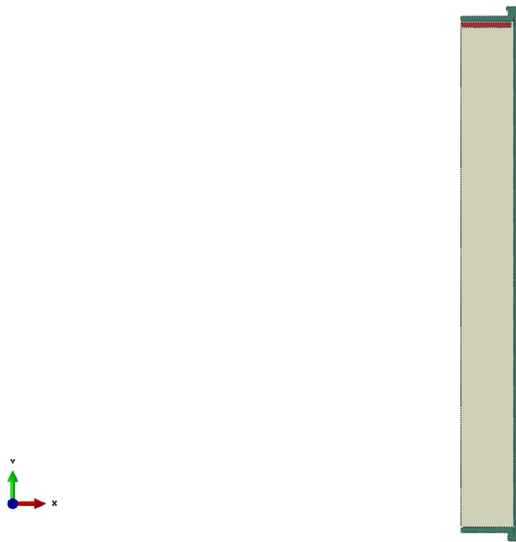
Figure 3-1. *Plot showing the geometry for the axi-symmetric model. Insert (grey), insert lid (red) and copper shell (green).*
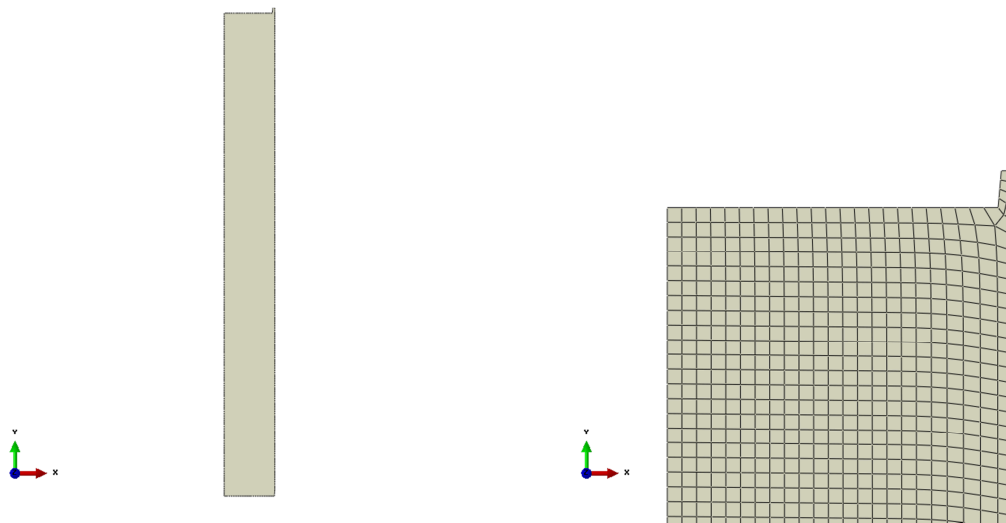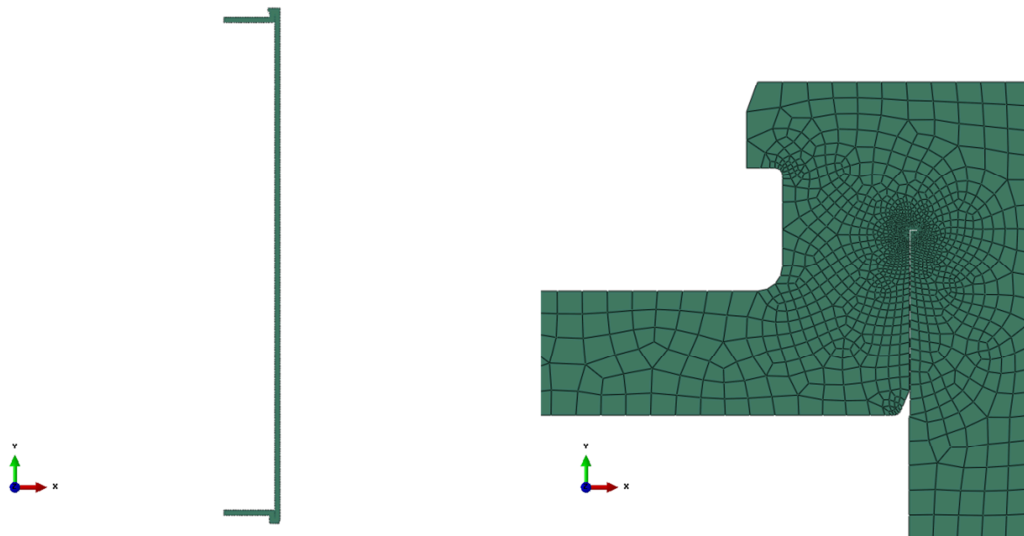
Figure 3-2. *Plot showing the geometry for the insert (left) and detail of the mesh (right).*
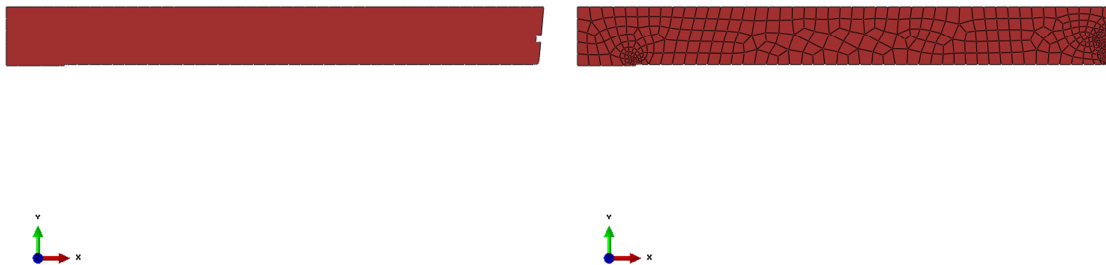
Figure 3-3. *Plot showing the geometry for the steel lid (left) and the mesh (right).*

Figure 3-4. *Plot showing the geometry for the copper shell (left) and detail of the mesh at the lid (right).*

4   Material models

The finite element code Abaqus (version 6.12, Dassault Systèmes Simulia Corp.) was used for the calculations. The materials have been modelled as elastic-plastic with stress-strain properties that correspond to each material and the applied shear load induced strain rate, when applicable. Note that in Abaqus values outside the definition range will be constant with the last value defined.

4.1   Nodular cast iron (insert)

The material model for the insert is based on a von Mises' material model with elastic behaviour defined by Young's modulus and the Poisson's ratio and the plastic behaviour defined through yield surface (true stress) versus plastic strain (defined as logarithmic strain), see Table 4-1 and Figure 4-1 "Dragprovning av gjutjärn" (SKBdoc 1201865).

The experiments were performed at 0 $^{\circ}$C.

Table 4-1. Stress-strain definition for the insert.

Plastic Strain (%)	True stress (MPa)			
	Strain rate=0/s	Strain rate= 2×10^{-4}/s	Strain rate=0.5/s	Strain rate factor at strain rate=0.5/s
0	293	293	348	1.19
1	324	324	367	1.13
2	349	349	385	1.10
3	370	370	406	1.10
4	389	389	423	1.09
5	404	404	438	1.09
6	418	418	451	1.08
7	428	428	464	1.08
8	438	438	474	1.08
9	447	447	483	1.08
10	456	456	490	1.07
11	465	465	498	1.07
12	472	472	504	1.07
13	478	478	510	1.07
14	484	484	516	1.07
15	488	488	520	1.07
16	491	491	521	1.06

The strain rate dependency is defined by assuming that the yield surface is proportional to the strain rate factor (at the strain rate 0.5/s the factor 1.08 has been chosen and at strain rate 0/s the factor is 1.0).The instantaneous strain rate factor is then linearly interpolated between 1 and 1.08 using the instantaneous strain rate. Values above 16% plastic strain are not available (none of the performed analyses have plastic strains outside the material definition).

The strain rate dependency is not needed in this study since the swelling process is very slow but is included in the existing material definition.

Furthermore, Young's modulus E = 166 GPa and Poisson's ratio ν = 0.32 (Raiko et al. 2010).
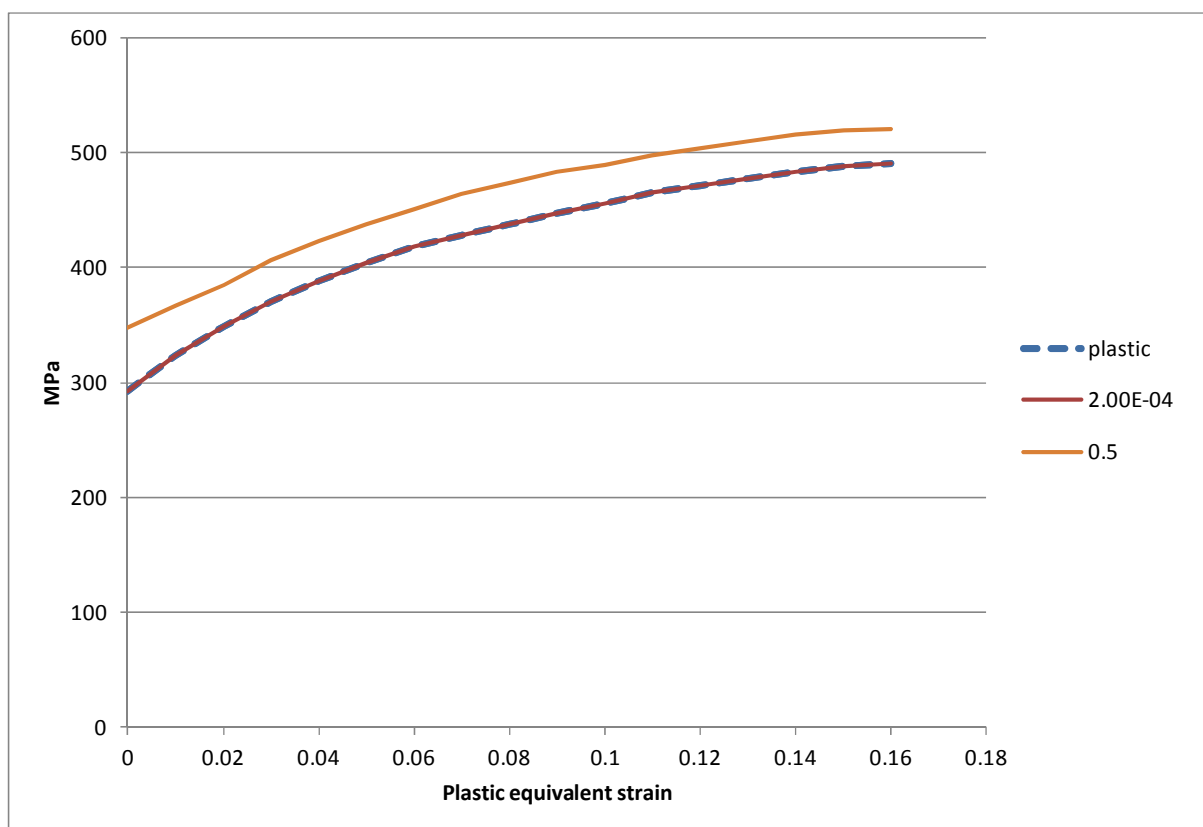
Figure 4-1. *Insert yield surface, true stress [MPa], versus logarithmic plastic equivalent strain for different plastic strain rates. Note that the base (plastic) is defined to coincide with strain rate= $2x10^{-4}/s$.*

4.2   Steel (insert lid)

The material model for the insert lid is based on a von Mises' material model with elastic behaviour defined by Young's modulus and the Poisson's ratio. The plastic behaviour is defined through yield surface (true stress) versus plastic strain (calculated as logarithmic strain).

Manufacturing drawings for the lid specify steel S355J2G3. Strain versus stress for steel Domex 355 MC B with Re = 389 MPa (yield stress) and Rm = 484 MPa (ultimate stress) can be found from SSABDirekt (2008). According to SS-EN 10025-2:2004, the material S355 with nominal thickness 40-63 mm has Re = 335 MPa (yield stress) and Rm = 470-630 MPa (ultimate stress). Scaling strain versus tensile stress curves for Domex 355 by the minimum values given in SS-EN 10025-2:2004 implies the simplified material definition (engineering data) shown in Table 4-2 and Figure 4-2. Only data for strains up to 20% are available but this is within the obtained strain levels for the performed analyses.

Table 4-2. Nominal stress-nominal strain definition for the insert lid.

Strain (%)	Stress (MPa)	Log Strain (%)	True Stress (MPa)
0	0	0	0
0.1595	335	0.1593	335
15	470	13.98	540
20	470	18.2	564

Furthermore, Young's modulus E = 210 GPa and Poisson's ratio ν = 0.3 according to Raiko et al. (2010, Table 4-2).
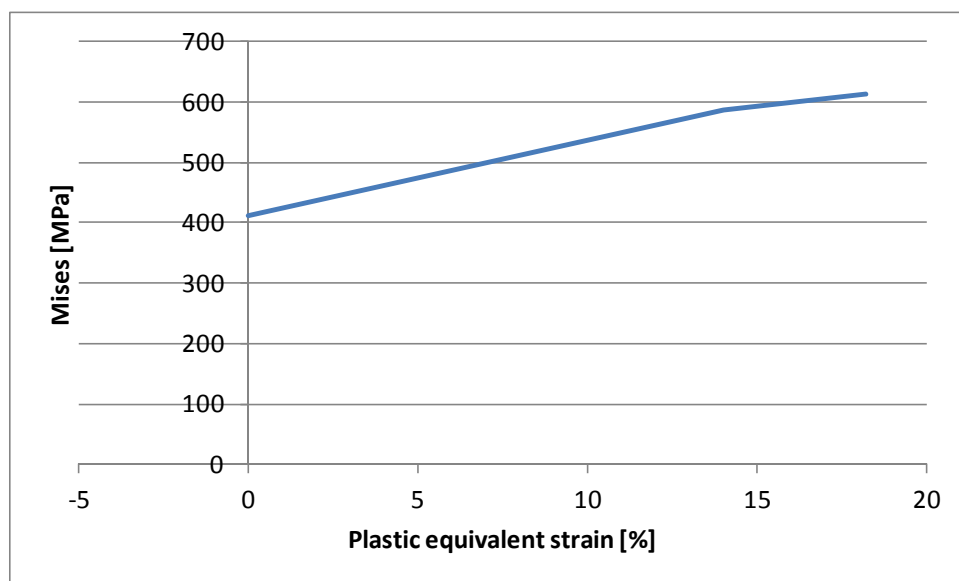
Figure 4-2. *Insert lid yield surface, true stress [MPa], as a function of the logarithmic plastic equivalent strain.*

The data with lowest value from the experiments (SS-EN 10025-2:2004) has been chosen for the yield surface. However, the plasticity definition for the insert lid has very minor influence on the overall results.

4.3   Copper model

The tensile stress-strain properties of the copper in the copper shell were investigated by the Corrosion and metals research institute, Kimab, and the results were then represented by a creep material model developed by Rolf Sandström, see Sandström and Andersson (2008), Jin et al. (2008) and Sandström et al. (2009).

The material model for the short duration analysis (neglecting creep) is based on a simplified elastic-plastic model, see Table 4-3, using data from the creep model assuming a strain rate of 5×10^{-3}/s.

The flow curve data has been calculated from Sandström et al. (2009) wherein eq.(17) has been used together with the parameter values defined in the corresponding Table 4-2, as well as m = 3.06, α = 0.19, ω = 14.66.

The copper model data is shown in Figure 4-3.

Table 4-3. Elastic-plastic material data for the copper at strain rate 5×10^{-3}/s.

Elastic part		Plastic part: von Mises stress σ_j (MPa) at the following plastic strains (ε_p)					
E (MPa)	ν	0	0.10	0.20	0.30	0.40	0.50
$1.2 \cdot 10^5$	0.308	72	178	235	269	288	300
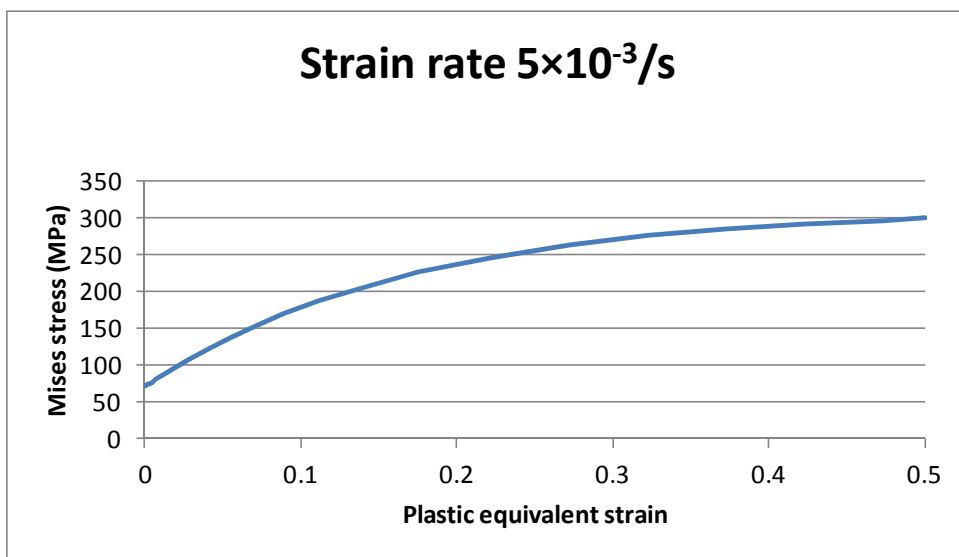
Figure 4-3. *Copper shell yield surface, true stress [MPa], as a function of the logarithmic plastic equivalent strain at strain rate $5x10^{-3}/s$.*

5   Contact definitions

All the boundaries of the insert and the insert lid interact through contact surfaces allowing finite sliding. All contact surfaces have friction at sliding with no cohesion and the friction coefficient 0.1, i.e. the friction angle (ϕ) is 5.7° and the cohesion (c) is 0 kPa.

The contact is released when the contact pressure is lost.

6   Boundary conditions and loading

Symmetry conditions have been specified for the symmetry plane (displacements in the normal direction to the symmetry plane prescribed to zero) and also the copper shell has prescribed zero displacements in the vertical direction at the base, see Fig 6-4. Figure 6-1 shows all loads (except the gravity load) and boundary conditions for the two cases studied. Figures 6-2 to 6-3 show details of loads and boundary conditions. The buffer swells in vertical direction from the bottom of the rock but the analyses are simplified by replacing the buffer with corresponding stresses on the copper shell (pressure and shear stresses). The upper part of the canister has shear stresses directed upwards and the lower part shear stresses directed downwards. The displacement of the canister is calculated relative to the bottom right corner (which thus is fixed).
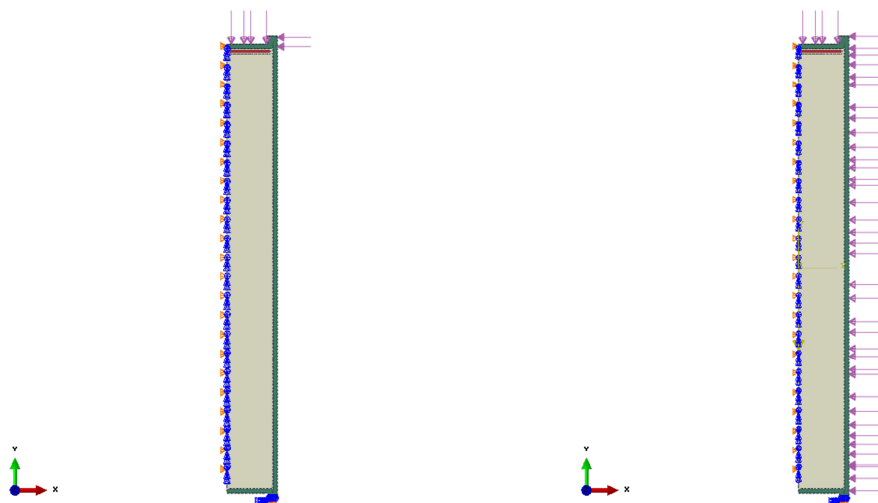
Figure 6-1. *Plot showing prescribed boundary conditions (blue and orange symbols) and applied loads (arrows). Left plot shows the case with radial and axial swelling pressure on the copper lid and outer top of the copper shell. Right plot shows the case with gravity and swelling pressure on the copper lid and the outer surface of the copper shell.*
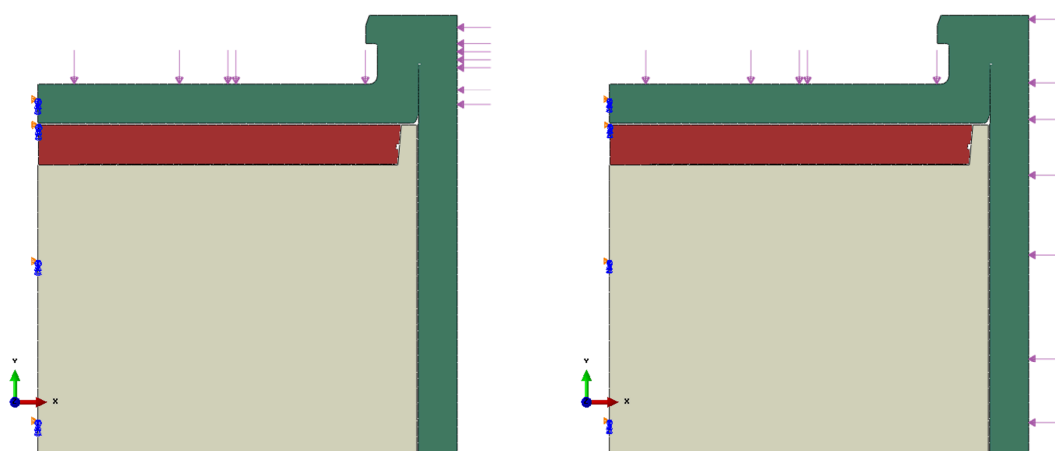
Figure 6-2. *Plot showing prescribed boundary conditions (blue and orange symbols) and applied loads (arrows). Left plot shows the case with swelling pressure on the copper lid and outer top of the copper shell, right plot shows the case with gravity and swelling pressure on the copper lid and the outer surface of the copper shell.*
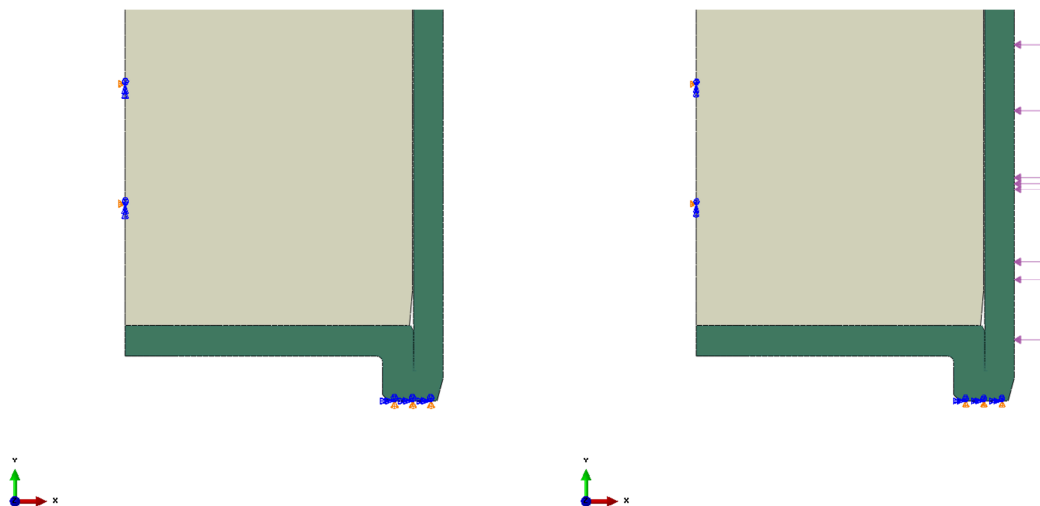
Figure 6-3. *Plot showing prescribed boundary conditions (blue and orange symbols) and applied loads (arrows). Left plot shows the case with swelling pressure on the copper lid and outer top of the copper shell, right plot shows the case with gravity and swelling pressure on the copper lid and the outer surface of the copper shell. Symmetry is defined by prescribed displacements in the normal direction (left) and the copper shell also is fixed at the bottom (right).*
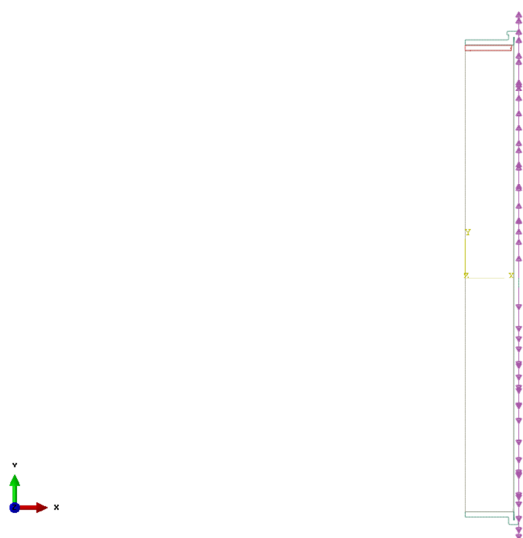
Figure 6-4. *Plot showing applied shear load caused by swelling of the buffer. Note the difference in direction, upward for top half and downward for bottom half, for the case with gravity and swelling pressure on the copper lid and the outer surface of the copper shell.*

Svensk Kärnbränslehantering AB
Swedish Nuclear Fuel and Waste Management Co

7 Analysis approach

The numerical calculations are performed using the FE-code Abaqus (version 6.12, Dassault Systèmes Simulia Corp.) assuming non-linear geometry and material definitions. This means that all non-linearities defined by the input will be considered such as large displacements, large deformations, non-linear interactions (contact) and non-linear materials. All non-linear contributions will be used when forming the equations to be solved for each equilibrium iteration. Short term analysis is based on static response but the results will depend on the time used for the simulation since rate-dependent material data is used. The code will choose suitable time-increments for the loading based on (in most cases) default convergence tolerances.

8 Results

For each analysis a large amount of results are available and to have an indication only a few values are reported:

- Appendix 1 shows results for Isostat_radial_pressure1
- Appendix 2 shows results for Isostat_radial_pressure2

The swelling pressure in the buffer is assumed to be build up by water originating from nearby cracks in the rock – the location of these cracks could be arbitrarily and thus the swelling process of the buffer are analyzed by studying two simplified cases which are assumed to represent the worst cases regarding the stress/strain magnitude in the copper shell. Below, the results for these cases are compared regarding Mises stress, hydrostatic pressure and equivalent plastic strain (PEEQ).

Figure 8-1 shows the comparison for Mises stress and Figure 8-2 shows the comparison for the hydrostatic pressure. As can be seen the case with swelling pressure at the outer surface of the copper shell combined with vertical shear stresses implies highest values which occur in the steel lid. Maximum Mises stress for the two cases is 481 and 498 MPa, respectively, and corresponding maximum hydrostatic pressure is 705 and 718 MPa.
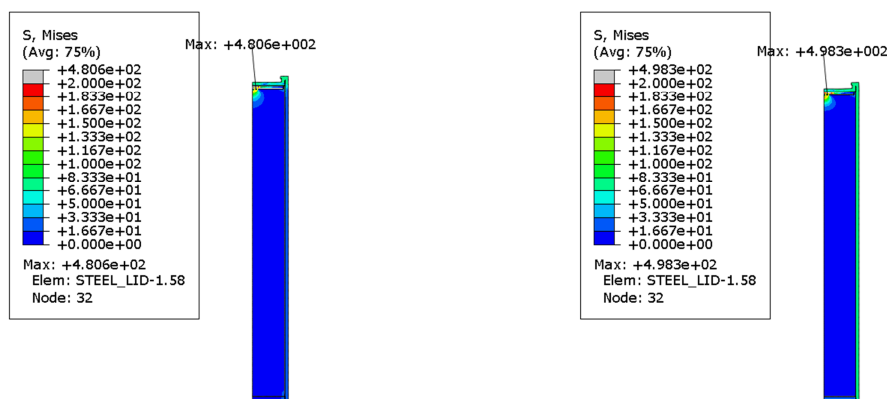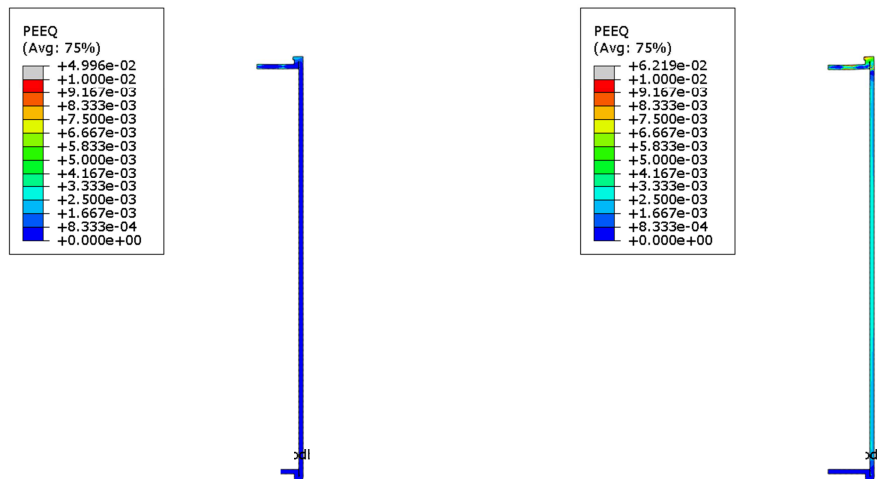

Figure 8-1. *Mises stress [MPa] in the canister. Swelling pressure only applied at the top (left) and swelling pressure applied at the top and swelling pressure and shear stress applied at the outer copper shell surface (right). Maximum value occurs in the steel lid.*

Svensk Kärnbränslehantering AB
Swedish Nuclear Fuel and Waste Management Co
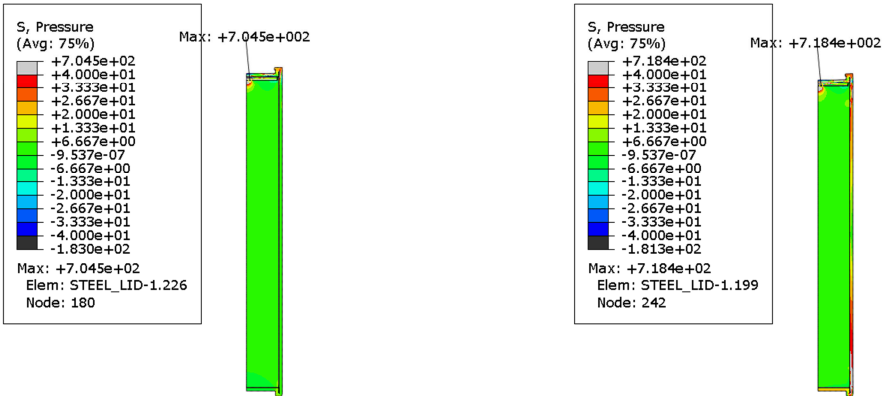
Figure 8-2. *Hydrostatic pressure [MPa] in the canister. Swelling pressure only applied at the top (left) and swelling pressure applied at the top and swelling pressure and shear stress applied at the outer copper shell surface (right). Maximum hydrostatic pressure occurs in the steel lid.*

Figures 8-3 to 8-5 show the comparison for the equivalent plastic strain (PEEQ) in the copper shell. As can be seen the highest values occur when the shear stress caused by swelling of the buffer is considered (6.2 and 5%, respectively). Maximum PEEQ occurs in the bottom weld of the copper shell but also the top of the copper shell has higher magnitude for this case since the support from the insert is lost. Figures 8-6 and 8-7 show that the hydrostatic pressure is positive for regions with high equivalent plastic strain.

Figure 8-3. *Equivalent plastic strain (PEEQ) in the copper shell. Swelling pressure only applied at the top (left) and swelling pressure applied at the top and swelling pressure and shear stress applied at the outer copper shell surface (right).*
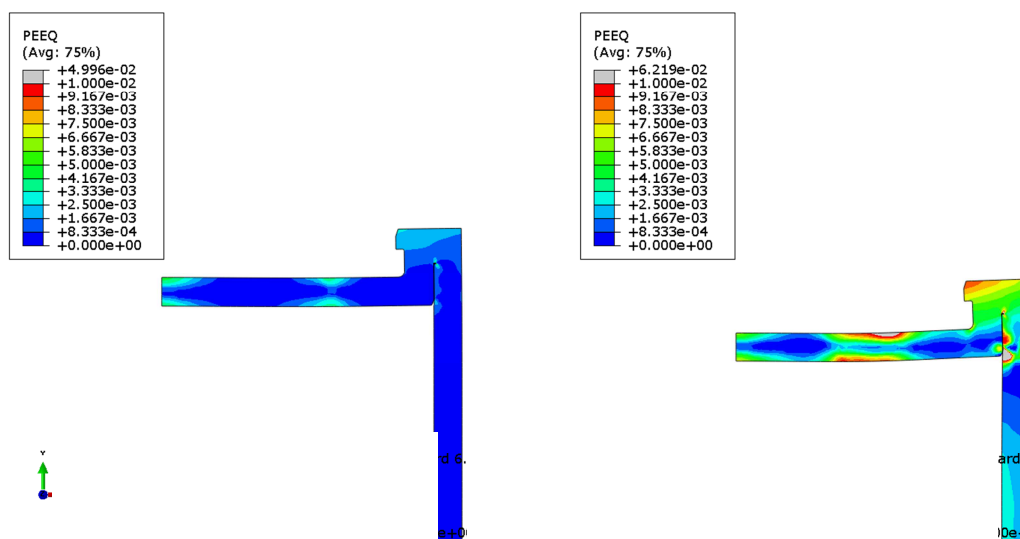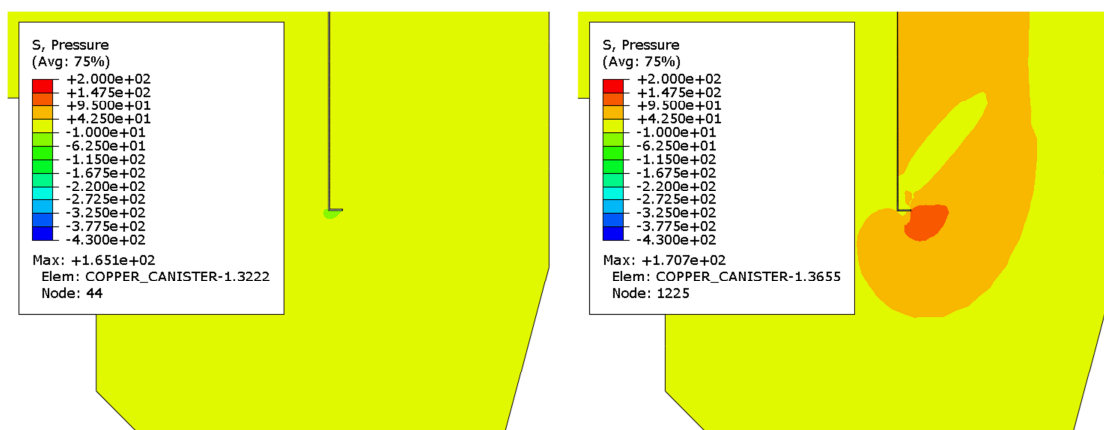

Figure 8-4. *Equivalent plastic strain (PEEQ) in the copper shell top. Swelling pressure only applied at the top (left) and swelling pressure applied at the top and swelling pressure and shear stress applied at the outer copper shell surface (right).*

Svensk Kärnbränslehantering AB
Swedish Nuclear Fuel and Waste Management Co
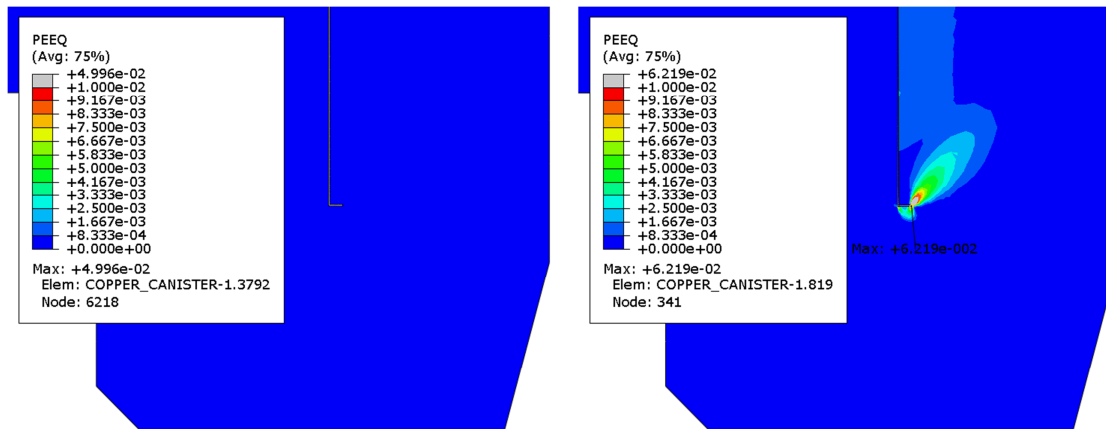
Figure 8-5. *Equivalent plastic strain (PEEQ) in the copper shell base. Swelling pressure only applied at the top (left) and swelling pressure applied at the top and swelling pressure and shear stress applied at the outer copper shell surface (right).*
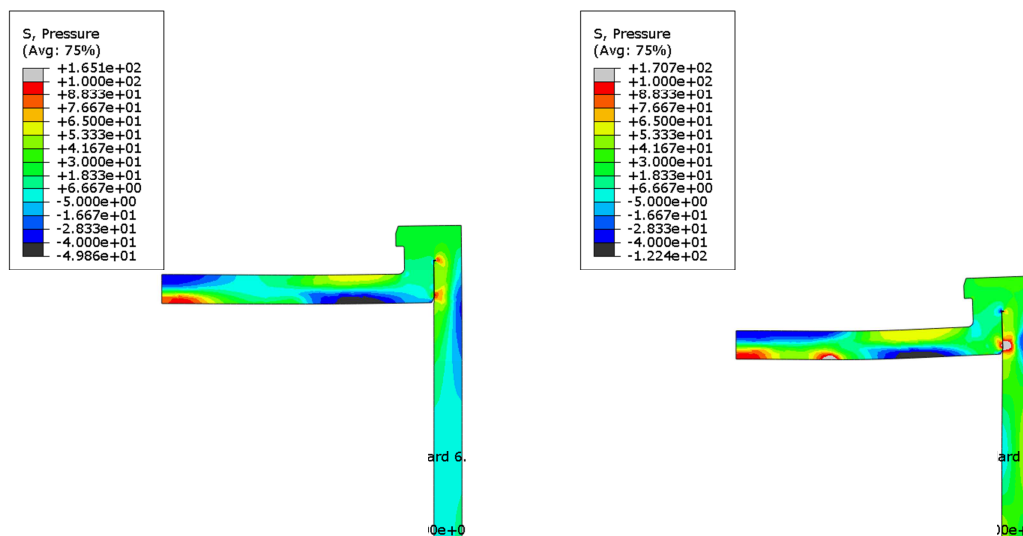
Figure 8-6. *Hydrostatic pressure in the copper shell top. Swelling pressure only applied at the top (left) and swelling pressure applied at the top and swelling pressure and shear stress applied at the outer copper shell surface (right).*

Note that the plots have same scaling for comparison reasons (see also Appendix 1 and 2 where the scaling is made so that the actual distribution is more clearly visible. Maximum equivalent plastic strain (PEEQ) is 6.2% for "worst case scenario" and is in a region with compressive stresses.

Svensk Kärnbränslehantering AB
Swedish Nuclear Fuel and Waste Management Co

Figure 8-7. *Hydrostatic pressure in the copper shell bottom. Swelling pressure only applied at the top (left) and swelling pressure applied at the top and swelling pressure and shear stress applied at the outer copper shell surface (right).*

Figure 8-8 shows a comparison of the equivalent plastic strain in the steel lid. As can be seen the two cases show very similar values. Maximum equivalent plastic strain is 10.6 and 11.6%, respectively, and occurs at the geometric discontinuity of the steel lid. This is consistent with the results for Mises stress.

However, the purpose of showing stresses and strains in the steel lid is mainly to confirm that they depend on the swelling pressure at the copper lid and that bending energy in the copper shell affects the amount of load transferred from the copper shell to the steel lid. The actual magnitude of equivalent plastic strain exhibits very local plasticity and depends on how accurate the geometric change is modelled.
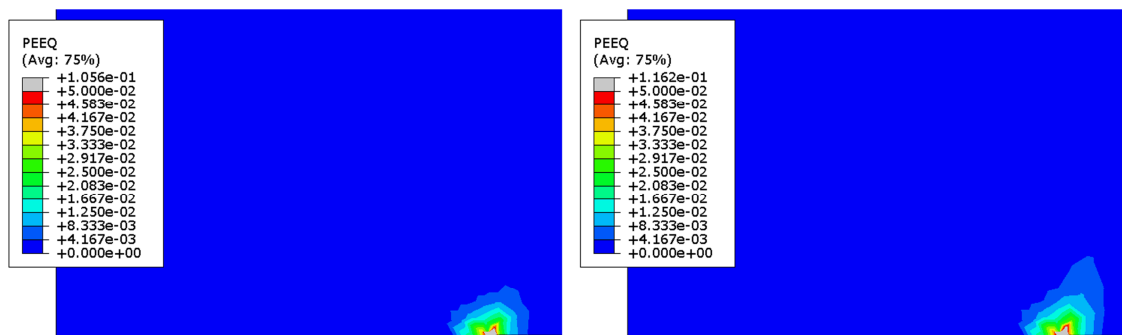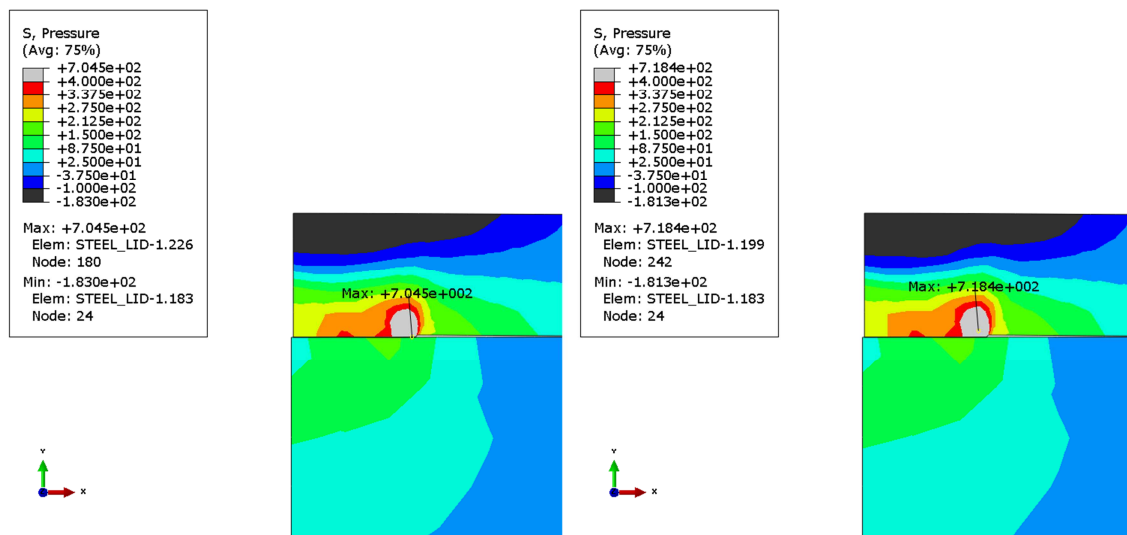

Figure 8-8. *Equivalent plastic strain (PEEQ) in the steel lid. Swelling pressure only applied at the top (left) and swelling pressure applied at the top and swelling pressure and shear stress applied at the outer copper shell surface (right).*

Figures 8-9 to 8-11 show the Mises stress, hydrostatic pressure and equivalent plastic strain at the contact zone between the steel lid and the insert. The highest values are in the steel lid (Mises 481 MPa and 498 MPa, hydrostatic pressure 705 and 718 MPa, equivalent plastic strain 10.6 and 11.6 %, respectively, for the two cases). The extreme values are at the geometric discontinuity and are very localized.

PDF rendering: DokumentID 1419643, Version 1.0, Status Godkänt, Sekretessklass Öppen
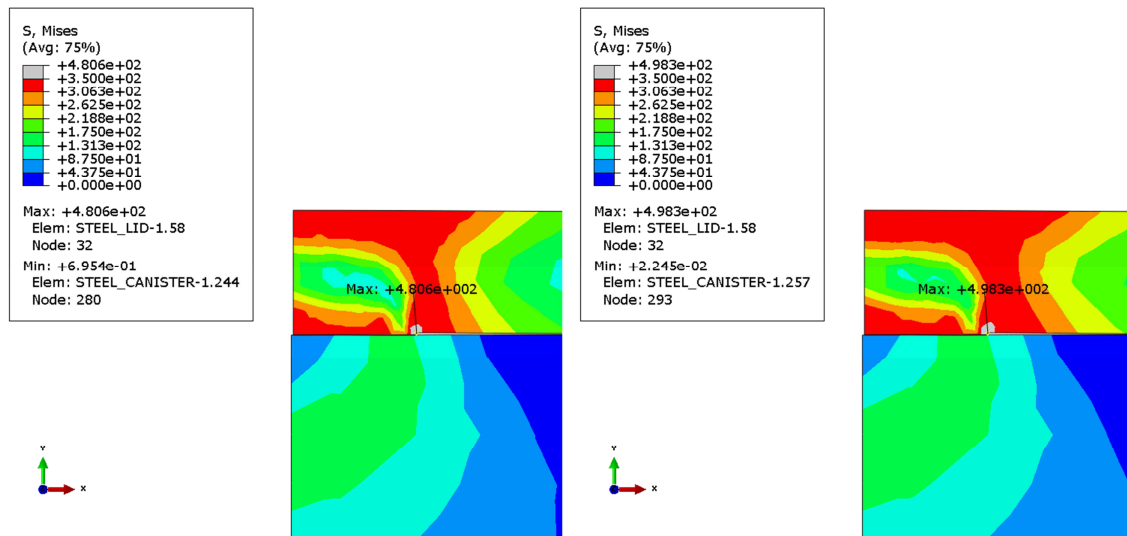
Figure 8-9. *Mises stress in the steel lid and the insert. Swelling pressure only applied at the top (left) and swelling pressure applied at the top and swelling pressure and shear stress applied at the outer copper shell surface (right).*

Figure 8-10. *Hydrostatic pressure in the steel lid and insert. Swelling pressure only applied at the top (left) and swelling pressure applied at the top and swelling pressure and shear stress applied at the outer copper shell surface (right).*
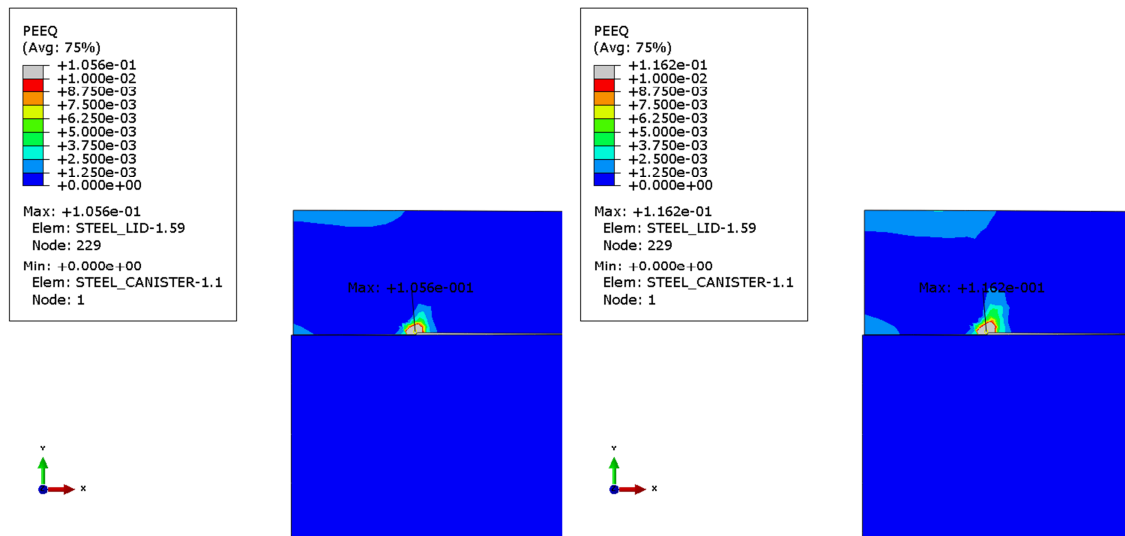
Figure 8-11. *Equivalent plastic strain (PEEQ) in the steel lid and insert. Swelling pressure only applied at the top (left) and swelling pressure applied at the top and swelling pressure and shear stress applied at the outer copper shell surface (right).*

9 Uncertainties

The obtained results are based on several assumptions regarding loads and material properties. Also the discretization in the computer model will affect the results. Some of these influencing factors are addressed below:

- Strain rate effects in the copper and iron will affect the results. The copper shell has the strain rate effect included for all reported analyses.

- All experiments used for material calibration have a spread which will imply a range for the properties defining each material model.

- Element mesh is rather fine but nevertheless it is too coarse in some regions, especially at the welds and regions with geometric discontinuities. A more refined mesh will probably increase the maximum stress and strain levels. Fortunately, the use of non-linear material properties (such as plasticity and creep) will decrease the sensitivity to the used mesh. The used mesh has been judged to be accurate enough. Since several models have been executed with different mesh densities it has been possible to compare and the conclusion is that the mesh in a global sense is accurate.

10 Evaluation and conclusions

- The equivalent plastic strain (PEEQ) for the case with radial and axial swelling pressure only applied at the top of the copper shell is rather low (about 5%). When swelling of the buffer is considered and combined with the swelling pressure the equivalent plastic strain increases to about 6.2% but should not cause any failure of the copper shell since the ductility is at least 50% for time independent plastic for copper, see Figure 4-3.

- The highest equivalent plastic strain occurs where the hydrostatic pressure is positive.

Svensk Kärnbränslehantering AB
Swedish Nuclear Fuel and Waste Management Co

- The performed analyses show no indication for failure in the copper shell not even when the most pessimistic assumptions are made.

References

Börgesson L, Dueck A, Johannesson L-E, 2010. Material model for shear of the buffer – evaluation of laboratory test results. SKB TR-10-31, Svensk Kärnbränslehantering AB.

Jin L-Z, Sandström R, 2008. Creep of copper canisters in power-law breakdown. Computational Materials Science 43, 403–416.

Raikko H, Sandström R, Rydén H, Johansson M, 2010. Design analysis report for the canister. SKB TR-10-28, Svensk Kärnbränslehantering AB.

Sandström R, Andersson H C M, 2008. Creep in phosphorus alloyed copper during power-law breakdown. Journal of Nuclear Materials 372, 76–88.

Sandström R, Hallgren J, Burman G, 2009. Stress strain flow curves for Cu-OFP. SKB R-09-14, Svensk Kärnbränslehantering AB.

SSABDirekt, 2008. Steelfacts Domex 355 MC. Available at http://www.ssabdirect.com. [19 September 2008].

SS-EN 10025-2:2004. Varmvalsade konstruktionsstål – Del 2: Tekniska leveransbestämmelser för olegerade stål (Hot rolled products of structural steels - Part 2: Technical delivery conditions for non-alloy structural steels). Stockholm: Swedish Standards Institute.

Unpublished documents

SKBdoc id, version	Title	Issuer, year
1201865, ver 1.0	Dragprovning av gjutjärn. (In Swedish.)	KTH, 2009
1203875, ver 1.0	Ritningsförteckning för kapselkomponenter. (In Swedish.)	SKB, 2009

Appendix 1 – Isostat_radial_pressure1

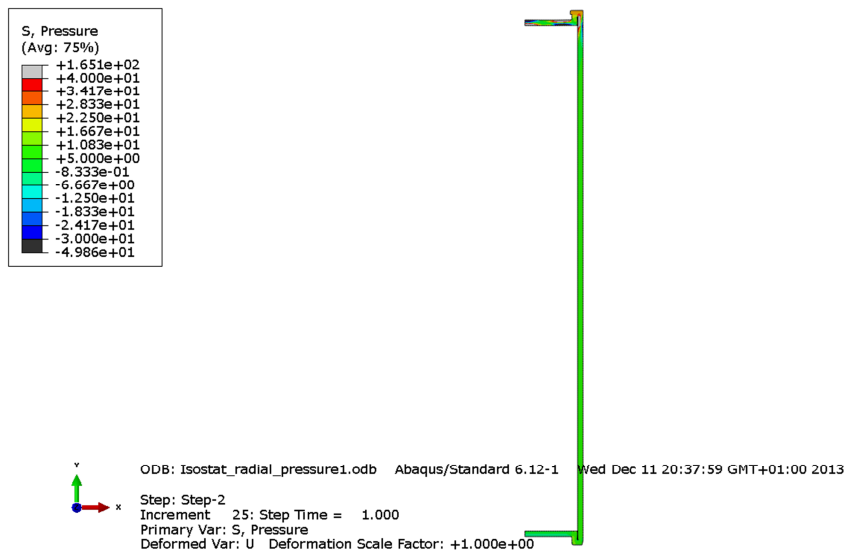Plots showing contours of pressure and equivalent plastic strain (PEEQ).

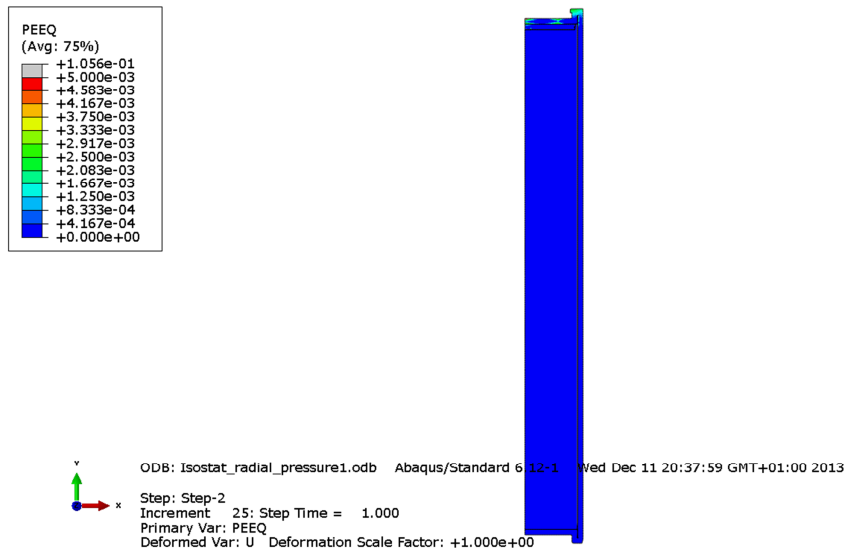**Figure A1-1.** *Plot showing hydrostatic pressure in the copper shell.*

Figure A1-2. *Plot showing equivalent plastic strain in the insert, steel lid and copper shell.*
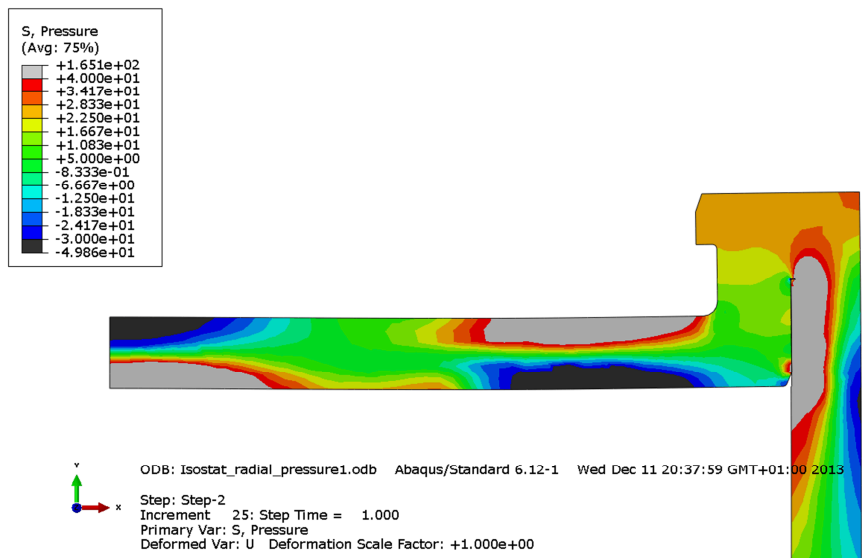
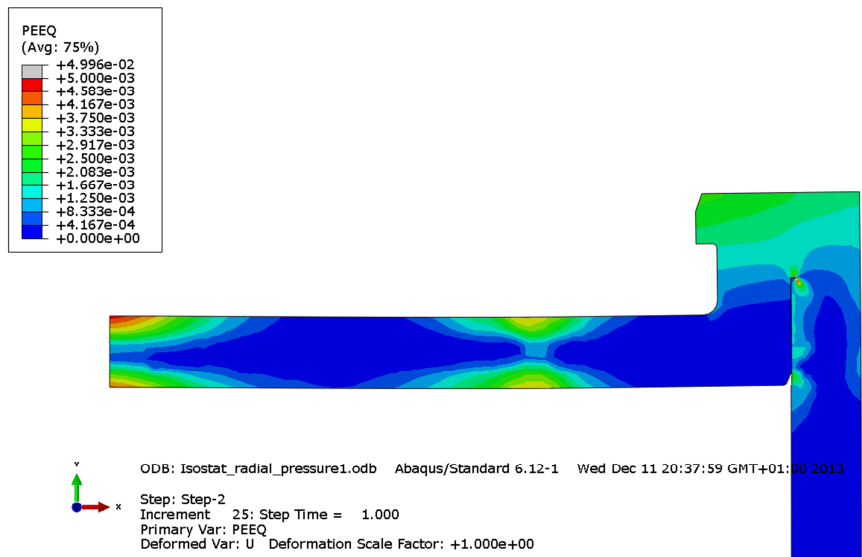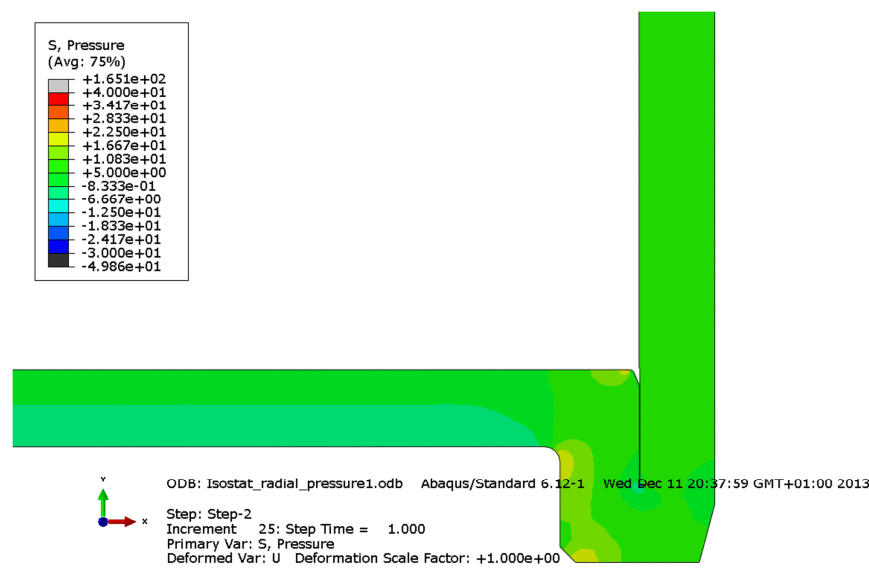**Figure A1-3.** Plot showing hydrostatic pressure in top of the copper shell.

Figure A1-4. *Plot showing equivalent plastic strain (PEEQ) in top of the copper shell.*

Figure A1-5. *Plot showing hydrostatic pressure in bottom of the copper shell.*
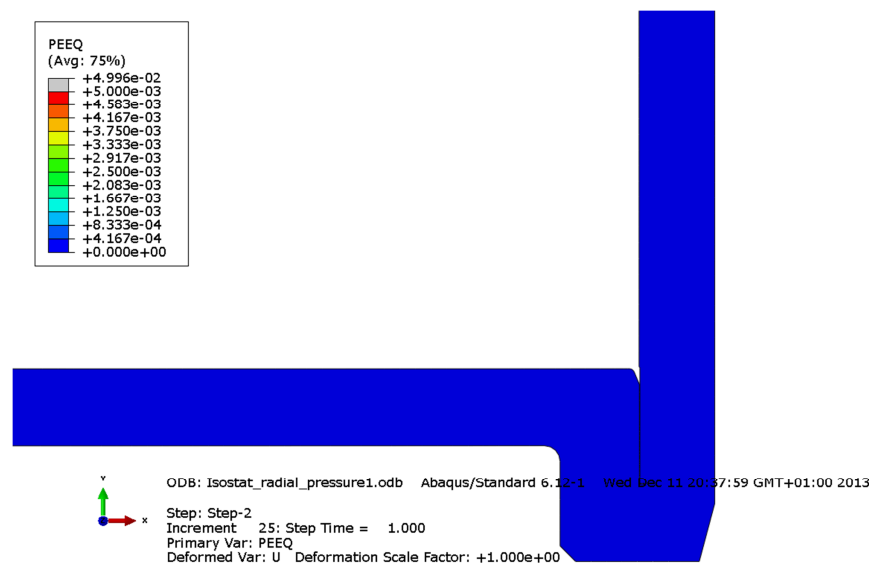

Figure A1-6. *Plot showing equivalent plastic strain (PEEQ) in bottom of the copper shell.*

Appendix 2 – Isostat_radial_pressure2

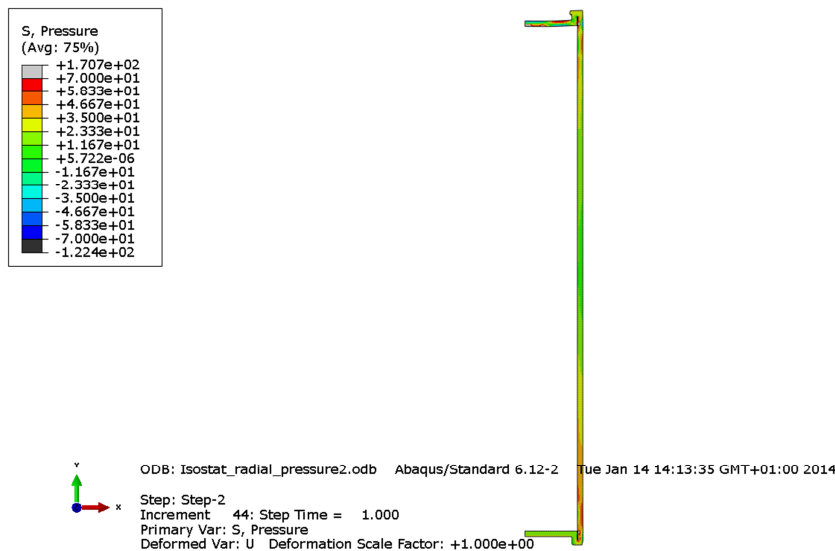Plots showing contours of pressure and equivalent plastic strain (PEEQ).

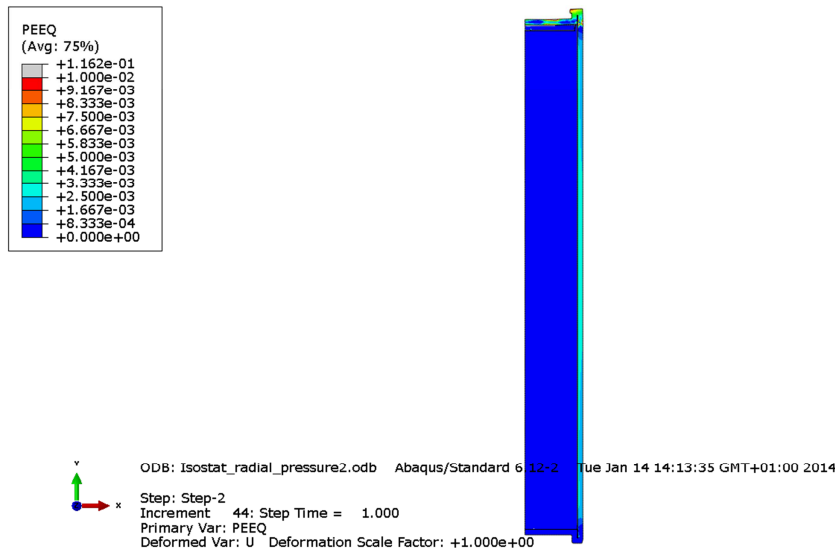**Figure A2-1.** *Plot showing hydrostatic pressure in the copper shell.*

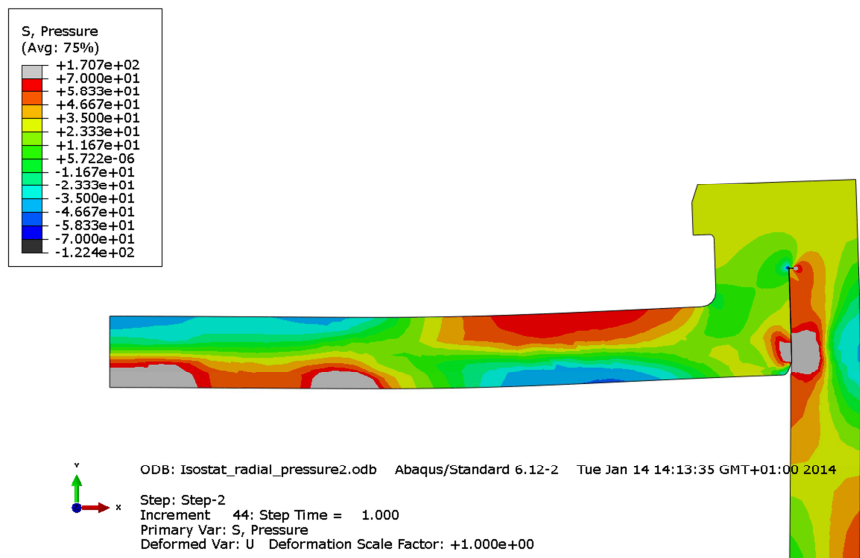**Figure A2-2.** *Plot showing equivalent plastic strain in the insert, steel lid and copper shell.*

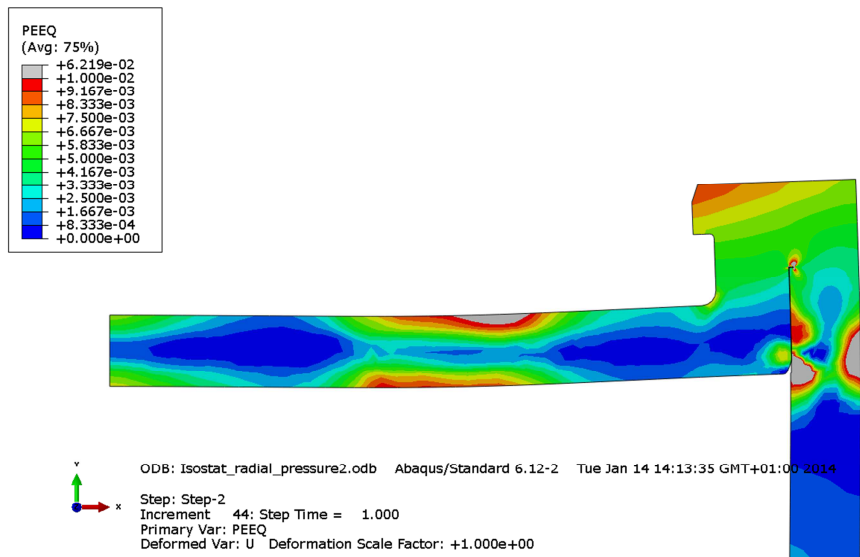**Figure A2-3.** *Plot showing hydrostatic pressure in top of the copper shell.*

Figure A2-4. *Plot showing equivalent plastic strain (PEEQ) in top of the copper shell.*
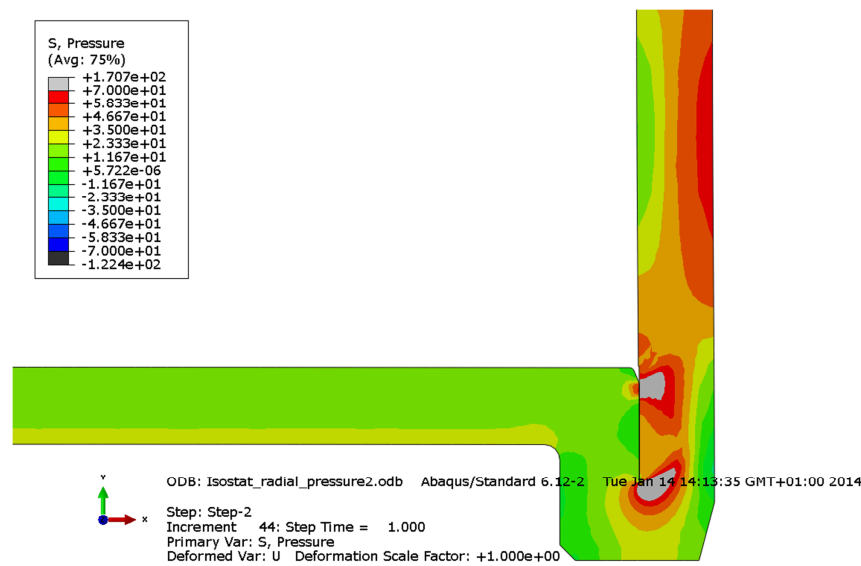
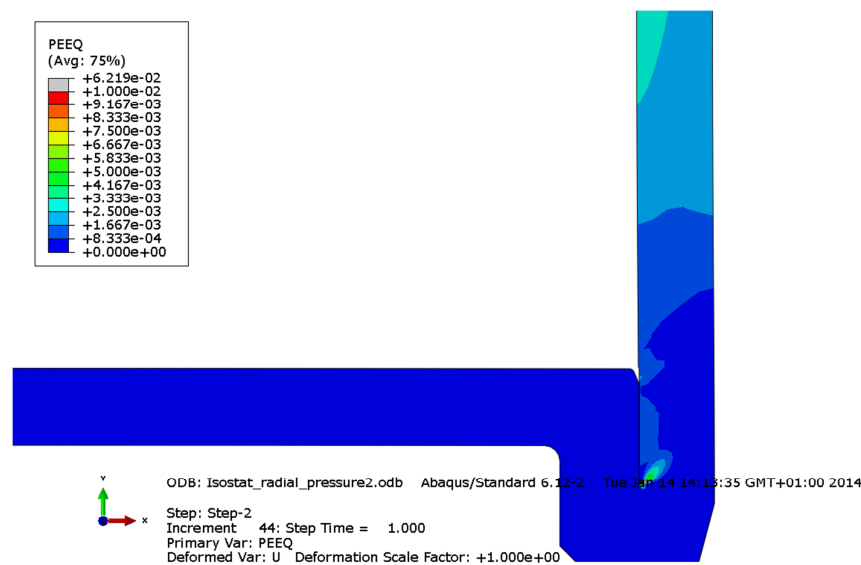**Figure A2-5.** *Plot showing hydrostatic pressure in bottom of the copper shell.*

Figure A2-6. *Plot showing equivalent plastic strain (PEEQ) in bottom of the copper shell.*

ODB: Isostat_radial_pressure2.odb   Abaqus/Standard 6.12-2   Tue Jan 14 14:13:35 GMT+01:00 2014

Step: Step-2
Increment   44: Step Time =   1.000

Deformed Var: U   Deformation Scale Factor: +1.000e+00
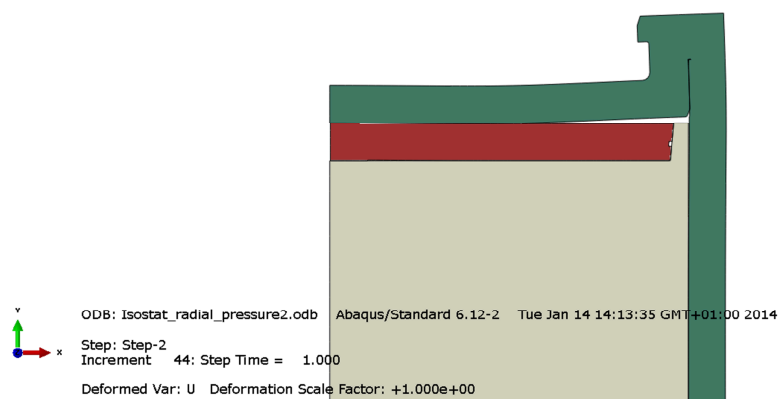
Figure A2-7. *Plot showing deformation at the top of the canister.*

Appendix 3 – Storage of files

This report is based on the results from a lot of FE-simulations using Abaqus which is a commercial available code and is thus not stored as part of the work. Below is a short description of files used in the project and directories for storage of these. These files are also stored at SKB.

The files are stored in directories as:

```
Geometry
Inputfiles
Plots
Analys av kapsel med ogynnsam trycklast.docx - this report
Scripts
```

1 – Plot-files used in the report

Contents in C:\Users\jhd\mappar\skb\ssm_questions\kapsel_integritet\Plots

Chapter 3
geometry_steel_lid.png
geometry_copper.png
geometry_bentonite.png
geometry_all.png

Chapter 7
loads4.png
loads3.png
loads2.png
loads1.png

Chapter 9
compare_peeq_copper2.png
compare_peeq_copper1.png
compare_peeq_steel_lid.png
compare_pressure.png
compare_mises.png
compare_deformed.png

Appendix 1
Isostat_radial_pressure1-pressure3.png
Isostat_radial_pressure1-peeq2.png
Isostat_radial_pressure1-pressure2.png
Isostat_radial_pressure1-peeq3.png
Isostat_radial_pressure1-pressure1.png
Isostat_radial_pressure1-peeq1.png

Appendix 2
Isostat_radial_pressure2-pressure3.png
Isostat_radial_pressure2-peeq2.png
Isostat_radial_pressure2-pressure2.png
Isostat_radial_pressure2-peeq3.png
Isostat_radial_pressure2-pressure1.png
Isostat_radial_pressure2-peeq1.png

2 – Input files used for the simulations

Each analysis is started by abaqus job=input-file (w/o .inp) user=creep_rs_march2009.

Files with extension "incl" are referenced by some of the input-files (extension "inp").

```
Contents in C:\Users\jhd\mappar\skb\ssm_questions\kapsel_integritet\InputFiles

Isostat_radial_pressure1.inp
Isostat_radial_pressure2.inp
```

4 – Scripts used for post-processing

Used inside ABAQUS/CAE or by abaqus cae startup=script.py after appropriate editing of job-name
inside the script-file.

```
Contents in C:\Users\jhd\mappar\skb\ssm_questions\kapsel_integritet\Scripts

geometry_loads.py                     - post processing file for geometry plots
compare.py               - post processing file for comparisons
post.py                          - post processing of results
```

5 – Geometry definitions

```
Contents in C:\Users\jhd\mappar\skb\ssm_questions\kapsel_integritet\Geometry

isostat_uneven.cae               - ABAQUS/CAE-database
isostat_uneven.jnl               - journal file
```